THE FASEB JOURNAL • RESEARCH • www.fasebj.org

Myoglianin triggers the pre-metamorphosis stage in hemimetabolan insects

Orathai Kamsoi and Xavier Belles[1]
Institute of Evolutionary Biology, Spanish National Research Council (CSIC)-Universitat Pompeu Fabra, Barcelona, Spain

ABSTRACT: Insect metamorphosis is triggered by a decrease in juvenile hormone (JH) in the final juvenile instar. What induces this decrease is therefore a relevant question. Working with the cockroach *Blattella germanica*, we found that myoglianin (Myo), a ligand in the TGF-β signaling pathway, is highly expressed in the corpora allata (CA, the JH-producing glands) and the prothoracic gland [(PG), which produce ecdysone] during the penultimate (fifth) nymphal instar (N5). In the CA, high Myo levels during N5 repress the expression of juvenile hormone acid methyl transferase, a JH biosynthesis gene. In the PG, decreasing JH levels trigger gland degeneration, regulated by the factors Krüppel homolog 1, FTZ-F1, E93, and inhibitor of apoptosis-1. Also in the PG, a peak of *myo* expression in N5 indirectly stimulates the expression of ecdysone biosynthesis genes, such as neverland, enhancing the production of the metamorphic ecdysone pulse in N6. The Myo expression peak in N5 also represses cell proliferation, which can enhance ecdysone production. The data indicate that Myo triggers the pre-metamorphic nymphal instar in *B. germanica* and possibly in other hemimetabolan insects.—Kamsoi, O., Belles, X. Myoglianin triggers the pre-metamorphosis stage in hemimetabolan insects. FASEB J. 33, 000–000 (2019). www.fasebj.org

KEY WORDS: juvenile hormone · ecdysone · corpora allata · prothoracic gland · MEKRE93 pathway

Insect metamorphosis is a fascinating phenomenon, but the master lines of its molecular regulatory mechanisms have only been elucidated recently. The process is controlled by 2 main hormones: ecdysone (where the best-known bioactive form is the derivative 20-hydroxyecdysone), which promotes the successive molts, and juvenile hormone (JH), which prevents the onset of metamorphosis in juvenile stages (1, 2). The molecular mechanisms underlying the action of these hormones are essentially based on the MEKRE93 pathway (3) that starts when JH binds to its receptor, methoprene-tolerant (Met), which belongs to the bHLH-PAS family of transcription factors (4). Upon binding to Met, JH triggers dimerization of Met with another bHLH-PAS protein, Taiman (Tai). The resulting JH-Met + Tai complex induces transcription of the target gene Krüppel-homolog 1 (*Kr-h1*), whose gene product represses the expression of *E93*, an ecdysone signaling-dependent gene whose gene product triggers metamorphosis (3, 5).

In hemimetabolan metamorphosis, exemplified by the German cockroach *Blattella germanica*, JH titers in the hemolymph rapidly decrease at the beginning of the final (sixth) nymphal instar (N6) (6). This is accompanied by a sudden drop of *Kr-h1* mRNA levels (7) as a result of the decrease in JH and the action of microRNA miR-2, which scavenges *Kr-h1* transcripts (8, 9). Consequently, *E93* becomes de-repressed and its expression increases, which triggers the onset of metamorphosis (3). These observations and knowledge of the MEKRE93 pathway are robust but lead to the following key question: What triggers the decrease in JH at the beginning of N6? Because we believe the answer lies in the penultimate (fifth) nymphal instar (N5), we searched for candidate genes in a series of transcriptomes prepared and sequenced in our laboratory, which covered the entire ontogeny of *B. germanica* (10). The analyses revealed that one of the most highly expressed genes in N5 is myoglianin (*myo*) (10).

Myoglianin (Myo) was discovered in *Drosophila melanogaster* as a new member of the TGF-β signaling pathway closely related to the vertebrate muscle differentiation factor myostatin. Expression studies led to the detection of maternally derived myo transcripts and of Myo expression in glial cells in midembryogenesis and, subsequently, in the developing somatic and visceral muscles and cardioblasts (11). Myo is a ligand in the activin branch of

ABBREVIATIONS: CA, corpora allata; CC–CA, corpora cardiaca–corpora allata complex; Cdk, cyclin-dependent kinase; Cyc, cyclin; Dap, dacapo; dib, disembodied; dsMock, control double stranded RNA; dsMyo, double-stranded RNA targeting myoglianin; dsRNA, double-strand RNA; EdU, 5-ethynyl-2′-deoxyuridine; JH, juvenile hormone; *jhamt*, juvenile hormone acid methyl transferase; Kr-h1, Krüppel homolog 1; Met, methoprene-tolerant; Myo, myoglianin; nvd, neverland; PG, prothoracic gland; *phm*, phantom; RNAi, RNA interference; sad, shadow; Smox, Smad on X

[1] Correspondence: Institute of Evolutionary Biology (CSIC-Universitat Pompeu Fabra), Passeig Marítim de la Barceloneta 37, 08003 Barcelona, Spain. E-mail: xavier.belles@ibe.upf-csic.es

doi: 10.1096/fj.201801511R
This article includes supplemental data. Please visit *http://www.fasebj.org* to obtain this information.

the TGF-β signaling pathway (12). In the context of metamorphosis, Myo has been shown to play a crucial role in the remodeling of the mushroom bodies in the larva–pupa transition of *D. melanogaster*, an action mediated by increased expression of the ecdysone receptor B1 (*EcR-B1*) gene in neural tissues (13). Regarding hemimetabolan insects, in the corpora allata (CA, the JH-producing glands) of the cricket *Gryllus bimaculatus*, Ishimaru *et al.* (14) showed that Myo inhibits the expression of juvenile hormone acid methyl transferase (*jhamt*), a gene coding for the last and crucial enzyme in the JH biosynthetic pathway. Reduction of the levels of this enzyme in the final nymphal instar triggers a decrease of JH production and commits the cricket to metamorphose (14). The findings of Ishimaru *et al.* (14) contrast with data reported in *D. melanogaster*, where the bone morphogenetic protein branch of the TGF-β signaling pathway promotes JH production by up-regulating the expression of *jhamt* (15).

Using *B. germanica* as a model, we found that Myo has functions beyond repressing the expression of *jhamt* in the CA during the transition from the penultimate to the final nymphal instar. We have also observed that Myo plays significant roles in the prothoracic gland [(PG), the ecdysone-producing gland] that help induce this transition and lead to the onset of metamorphosis. Our data indicate that Myo is an essential factor in terms of triggering the pre-metamorphosis stage in *B. germanica* and possibly in other hemimetabolan insects because it acts on the CA and the PG, the glands that produce the most important hormones regulating metamorphosis.

MATERIALS AND METHODS

Insects

The *B. germanica* cockroaches used in the experiments described herein were obtained from a colony fed Panlab (Harvard Apparatus, Holliston, MA, USA) dog chow and water *ad libitum* and reared in the dark at 29 ± 1°C and 60–70% relative humidity. Cockroaches were anesthetized with CO_2 prior to injection treatments, dissections, and tissue sampling.

RNA extraction and retrotranscription to cDNA

RNA extractions were carried out with the Gen Elute Mammalian Total RNA kit (MilliporeSigma, Madrid, Spain). A sample of 200 ng from each RNA extraction was used for mRNA precursors in the case of fat body, epidermis, and muscle. All the volume extracted of the corpora cardiaca–CA complex (CC–CA), PG, brain, and ovary was lyophilized in a freeze-dryer (ALPHA 1–2 LDplus; Thermo Fisher Scientific, Waltham, MA, USA) and resuspended in 8 μl of milli-Q H_2O (MilliporeSigma). RNA quantity and quality were estimated by spectrophotometric absorption at 260 nm in a spectrophotometer (ND-1000; NanoDrop Technologies, Wilmington, DE, USA). The RNA samples then were treated with DNase (Promega, Madison, WI, USA) and reverse transcribed with a First Strand cDNA Synthesis Kit (Roche, Basel, Switzerland) and random hexamer primers (Roche).

Determination of mRNA levels by real-time quantitative PCR

Real-time quantitative PCR was carried out in an iQ5 Real-Time PCR Detection System (Bio-Rad Laboratories, Hercules, CA, USA) using SYBRGreen (iTaq Universal SYBR Green Supermix; Applied Biosystems, Foster City, CA, USA). Reactions were performed in triplicate, and a template-free control was included in all batches. Primers used to study the transcripts of interest are detailed in Supplemental Table S1. The efficiency of each set of primers was validated by constructing a standard curve through 3 serial dilutions. Levels of mRNA were calculated relative to BgActin-5c mRNA (accession number AJ862721). Results are given as copies of the mRNA of interest per 1000 copies of BgActin-5c mRNA.

RNA interference

The detailed procedures for RNA interference (RNAi) assays have been described previously (16). The primers used to prepare the double-strand RNA (dsRNA) targeting *B. germanica* Myo are described in Supplemental Table S1. The sequence corresponding to the dsRNA [i.e., the double-stranded RNA targeting Myo (dsMyo)] was amplified by PCR and then cloned into a pST-Blue-1 vector. A 307 bp sequence from *Autographa californica* nucleopolyhedrosis virus (accession number K01149.1) was used as control dsRNA (dsMock). A volume of 1 μl of the dsRNA solution (3 μg/μl) was injected into the abdomen of freshly emerged fifth instar female nymphs (N5D0) or 1-d-old sixth instar female nymphs (N6D1) with a 5 μl Hamilton microsyringe. Control insects were treated at the same age with the same dose and volume of dsMock.

Morphologic studies of the PG

The PG was studied in female nymphs at chosen ages and instars. The gland was dissected out of the first thoracic segment of the animal under Ringer's saline, fixed in 4% paraformaldehyde in PBS for 1 h, washed with PBS 0.3% Triton, and incubated for 10 min in 1 mg/ml DAPI in PBS 0.3% Triton. The gland was mounted in Mowiol (Calbiochem, Madison, WI, USA) and observed with a fluorescence microscope (Axio Imager.Z1; Carl Zeiss AG, Oberkochen, Germany).

Experiments to measure cell proliferation in the PG

5-Ethynyl-2′-deoxyuridine (EdU) is a thymidine analog developed for labeling DNA synthesis and dividing cells *in vitro* (17), which is more sensitive and practical than the commonly used 5-bromo-2′-deoxyuridine. We followed an approach *in vivo*, using the commercial EdU compound Click-it EdU-Alexa Fluor 594 azide (Thermo Fisher Scientific), which was injected into the abdomen of the nymphs at chosen ages and instars with a 5 μl Hamilton microsyringe (1 μl of 20 mM EdU solution in DMSO). The control specimens received 1 μl of DMSO. The PG from treated specimens was dissected 1 h later and processed for EdU visualization according to the manufacturer's protocol.

RESULTS

Myo structure and expression in *B. germanica*

We obtained a cDNA of 1611 bp, comprising a complete open reading frame, by combining a Blast (*https://blast.ncbi.nlm.nih.gov/Blast.cgi*) search in *B. germanica* genome,

transcriptomic data, and PCR. Its conceptual translation gave a 537 aa protein (Supplemental Fig. S1) with significant similarity to the Myo sequence of other species, such as the fly *D. melanogaster* and the cricket *G. bimaculatus*, as described by Lo and Frasch (11) and Ishimaru *et al.* (14), respectively (Supplemental Fig. S2). As in other Myo orthologs, the full-length *B. germanica* Myo sequence contained the canonical RXXR processing site and 7 cysteines in the carboxy-terminal portion of the ORF, which correspond to the mature processed protein (Supplemental Figs. S1, 2).

To assess whether Myo was differentially expressed in different tissues, we measured its expression in brain, CC–CA, PG, ovary, fat body, epidermis, and muscle tissues in 3-d-old fifth instar female nymphs (N5D3) of *B. germanica*. PG showed the highest myo mRNA levels; a lower Myo expression was measured in brain, CC–CA, and muscle tissues; and the lowest expression was observed in fat body, ovary, and epidermal tissues (**Fig. 1*A***).

Because we were interested in the main hormones regulating metamorphosis (JH and ecdysone), we focused on the glands producing these hormones (the CC–CA complex and PG, respectively). Therefore, we determined the Myo expression pattern in these 2 glands during the fourth, fifth, and sixth (final) instar female nymphs (N4, N5, and N6). In the CC–CA, the highest expression was observed in N5, in accordance with the pattern we found in our previous transcriptome analyses (10). Within N5, maximal expression was found at the beginning of the instar (N5D0) (~500 mRNA copies per 1000 copies of actin mRNA) and progressively decreased until it practically vanished at the end of the instar (N5D6). During N6, Myo mRNA levels in the CC–CA were relatively low (10–50 mRNA copies per 1000 copies of actin mRNA) (Fig. 1*B*). In the PG, the highest Myo mRNA levels were also observed in N5, but expression peaked in the mid–late instar (N5D4, ~11,000 mRNA copies per 1000 copies of actin mRNA). The levels progressively decreased throughout the rest of the instar and N6, although they remained relatively high in N6 (~4000 mRNA copies per 1000 copies of actin mRNA) (Fig. 1*C*).

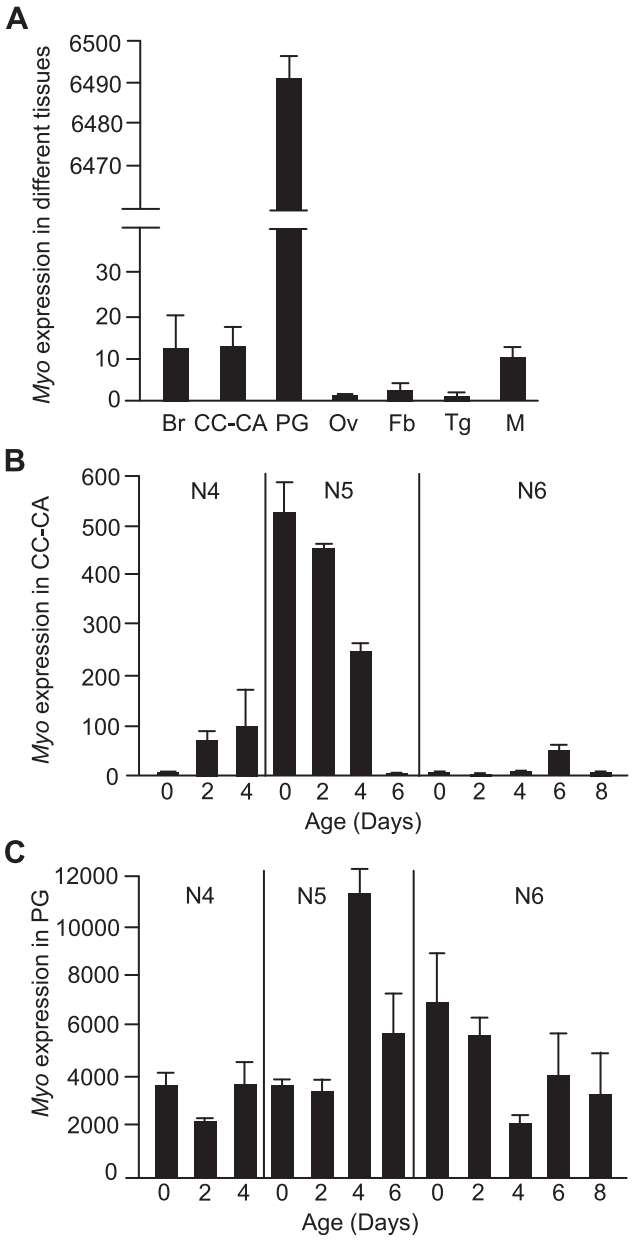

Figure 1. Expression of Myo in *B. germanica*. *A*) mRNA levels in brain (Br), CC–CA, PG, ovary (Ov), fat body (Fb), epidermis (tergites 2–7: Tg), and muscle (extensor muscle from the 6 femora pairs: M). Measurements were carried out on 3-d-old fifth-instar female nymphs. *B*) mRNA levels in CC–CA of fourth, fifth, and sixth instar female nymphs. *C*) mRNA levels in PG of fourth, fifth, and sixth instar female nymphs. Results are copies of *Myo* mRNA per 1000 copies of BgActin-5c mRNA and are expressed as the mean ± SEM (n = 3–5).

Myo depletion prevents metamorphosis

We used systemic RNAi to study the effects of Myo depletion on metamorphosis. We injected a single dose of 3 μg of dsMyo into the abdomen of N5D0 cockroaches. Controls were treated equivalently with the same dose of dsMock. In the CC–CA, Myo mRNA levels were significantly reduced in dsMyo-treated cockroaches (**Fig. 2*A***). When monitoring the experimental cockroaches up to the imaginal molt, we observed that all N5 controls (n = 44) molted to normal N6 after 6 d on average and then to normal adults 8 d later (Fig. 2*B*). The N5 dsMyo-treated cockroaches (n = 46) molted to N6 after 8 d on average; these N6 cockroaches had an apparently normal morphology but were smaller than the N6 controls (Fig. 2*C*, *D*). Of the 46 N6 dsMyo-treated cockroaches, 6 died and 40 molted to a supernumerary nymph (N7). Of the 40 N7 nymphs, 6 molted to the adult stage and 34 molted to a further supernumerary nymph (N8), which then molted to adults. A total of 28 of these adults presented a practically normal morphology (although they were slightly larger than control adults emerging from N6), whereas the wings and tegmina were somewhat separated in the other 6 adults (Fig. 2*D*). The supernumerary nymphal instars N7 and N8 lasted for ~8 d (Fig. 2*B*). We then examined the expression of genes involved in JH synthesis and signaling in the CC–CA at the beginning of N6. Results showed that the expression of *jhamt* and *Kr-h1* was significantly

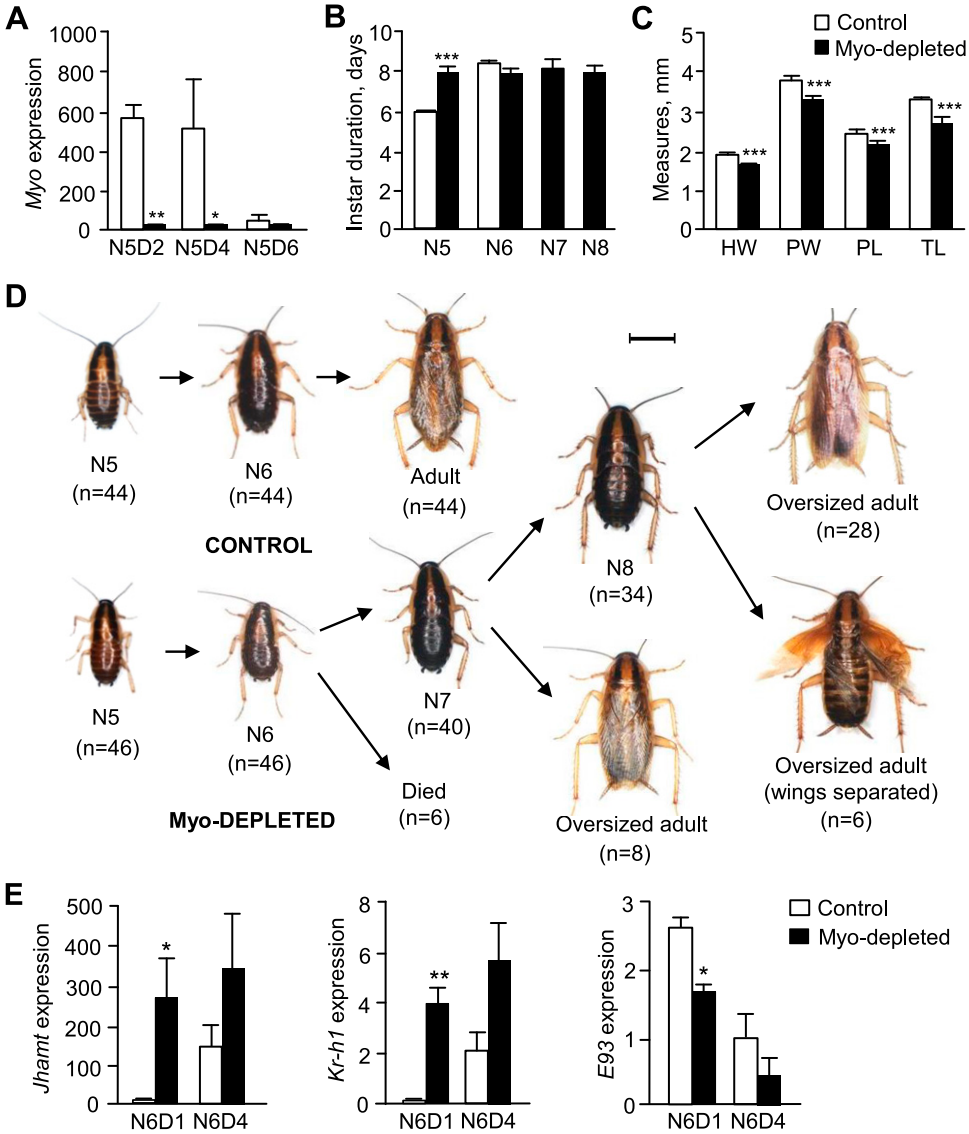

Figure 2. Effects of Myo mRNA depletion in the metamorphosis of *B. germanica*. *A*) mRNA levels of Myo in CC–CA of Myo-depleted cockroaches and in controls, measured on 2-, 4-, and 6-d-old fifth instar female nymphs (N5D2, N5D4, and N5D6). *B*) Duration (days) of N5 and N6 (and the supernumerary nymphal instars N7 and N8) in Myo-depleted cockroaches and in controls. *C*) Measures of morphologic parameters in N6 of Myo-depleted cockroaches and in controls. HW, head width; PL, pronotum length; PW, pronotum width; TL, metatibia length. *D*) Dorsal view of control and Myo-depleted cockroaches through successive molts. Freshly emerged fifth instar female nymphs (N5D0) were treated with dsMyo or with dsMock (control), and the morphology after the subsequent molts was examined. The number of specimens at the beginning of the experiments and after every molt is indicated. Scale bar, 4 mm. *E*) mRNA levels of *jhamt*, *Kr-h1*, and *E93* in CC–CA from dsMyo-treated cockroaches and controls on N6D1 and N6D4. In *A* and *E*, results are indicated as copies of the given transcript per 1000 copies of BgActin-5c mRNA. In all bar diagrams, results are expressed as the mean ± SEM (n = 3–5). Asterisks indicate statistically significant differences with respect to controls. $^*P < 0.05$, $^{**}P < 0.01$, $^{***}P < 0.001$ (Student's t test).

up-regulated, whereas that of *E93* was down-regulated (Fig. 2*E*).

In *D. melanogaster*, decapentaplegic, one of the ligands of the thick vein receptor of the bone morphogenetic branch of the TGF-β signaling pathway, which operates through the transcription factor Mothers against decapentaplegic (Mad), promotes JH production in the CA through up-regulating the expression of *jhamt* (15). In the cricket *G. bimaculatus*, Myo, which is a ligand of the Baboon receptor of the activin branch of the TGF-β signaling pathway that operates through the transcription factor Smad on X (Smox), inhibits JH production in the CA through down-regulating the expression of *jhamt* (14). Ishimaru *et al.* (14) proposed that the inhibitory action of Myo upon the expression of *jhamt* is mediated by a repression of the Mad effects. Depletion of Myo in the final nymphal instar of *G. bimaculatus* up-regulated *jhamt* expression; hence, JH production increased, and the crickets molted to supernumerary nymphs instead of adults (14). The results obtained in *B. germanica* are similar to those observed in *G. bimaculatus* in terms of metamorphosis phenotypes and the up-regulation of *jhamt* expression after Myo depletion. This is not surprising because both species are hemimetabolan and are closely related phylogenetically, that is, both belong to the "orthopteroid" group of the superorder Polyneoptera (18). Our results unveil the molecular mechanisms preventing metamorphosis, which are based on the MEKRE93 pathway (3). In the final nymphal instar, the *jhamt* up-regulation induced by Myo depletion led to an increase in *Kr-h1* expression, a JH-dependent factor that is the main transducer of the anti-metamorphic action of JH (7). Moreover, Kr-h1 represses *E93* (3), which is the master factor triggering metamorphosis (3, 19). In our Myo-depleted cockroaches, the up-regulation of *Kr-h1* expression explains the down-regulation of *E93* (Fig. 2*E*), whereas the observed reduction in *E93* expression explains why the cockroaches did not molt to the adult stage.

These observations are consistent with our previous work wherein we reported that the TGF-β/activin

signaling pathway contributes to the repression of *Kr-h1* expression and activation of *E93* expression during the metamorphosis of *B. germanica* (20). Because Myo signal is transduced by Smox and represses *jhamt* expression and JH production, one would expect that expression of the JH-dependent gene *Kr-h1* would be up-regulated if Smox were repressed, which is what was observed in our experiments (20). In the context of holometabolan metamorphosis, studies in *D. melanogaster* have shown that the TGF-β/activin branch is involved in wing disc patterning (21) and neuronal remodeling (22). Moreover, Gibbens *et al.* (23) have shown that the final larval stage of *D. melanogaster* was developmentally arrested when the TGF-β/activin pathway was blocked in the PG because the larvae were unable to produce the large pulse of ecdysone needed for metamorphosis. It has been demonstrated that Myo signaling through the TGF-β/activin pathway is crucial for mushroom body remodeling in the transition from the final larval stage to the pupa because it up-regulates neuronal *EcR-B1* expression (13). The same study revealed that myo-defective mutants can molt until the final larval stage and prepupate, but they become arrested before head inversion (13), which is consistent with the results reported by Gibbens *et al.* (23).

Myo depletion causes cell hyperproliferation in the PG

The PG of *B. germanica*, like in other cockroaches, has an X-shaped morphology, and its size varies during successive stages. Size variation roughly corresponds to the dynamics of ecdysone production because the most active glands have bigger secretory cells than the inactive glands (24). In the present work, we also studied the dynamics of cell proliferation in the PG during N5 and N6 using EdU labeling. In N5, which lasts for 6 d, we observed intense cell division between d 0 and 3 (the first 50% of the stage). In N6, which lasts for 8 d, intense cell division only occurred over d 0 and 1 (the first 12.5% of the stage) (**Fig. 3**). During these stages, the ecdysone pulse in N5 peaks sharply at around d 4, whereas in N6 ecdysone production follows a longer, shallower peak over d 5–7 (25). The nonoverlapping patterns of cell division and the ecdysone peak indicate that PG cells alternate between periods of cell proliferation and hormone synthesis, as occurs in other secretory glands, such as the CA (26). The form of the ecdysone pulse varies along the different molts; wider pulses appear to be characteristic of metamorphic molts (27). We believe the wide ecdysone pulse in N6, which triggers the metamorphic molt, requires an earlier and radical arrest of cell division, similar to the one observed in our Edu labeling observations (Fig. 3).

We used the same Myo-targeting RNAi experiment described above (3 μg of dsMyo injected in N5D0) to examine the effects in the PG. We found that Myo mRNA levels in the PG were significantly reduced in dsMyo-treated cockroaches compared with controls (**Fig. 4*A***). Preliminary dissections of Myo-depleted cockroaches in N5D4 and N6D4 revealed that PG size was greater than in controls (Fig. 4*B*). Measurement of the PG arm width during N5 and N6 showed that the PG from Myo-depleted cockroaches grew bigger than in the controls (Fig. 4*C*). Moreover, microscopic examination of the PG at high magnifications using Edu labeling revealed that Myo-depleted cockroaches exhibited much more active cell division than controls (Fig. 4*D*).

The transition from G1 into DNA replication (S phase) is crucial in determining whether to enter a new cell cycle, and 4 factors—cyclin (Cyc)E, CycA, dacapo (Dap), and cyclin-dependent kinase (Cdk)2—are key players in this transition. The accumulation of CycE and CycA, which form complexes with Cdk2, promotes the transition to the S phase, whereas Dap negatively regulates this transition, mainly by sequestering the CycE/Cdk2 complexes (28, 29). Moreover, in mouse C2C12 cells, myostatin, which is the Myo homolog in mammals (11), induces CycD degradation, resulting in cell cycle arrest (30). Based on these reports, we measured the expression of *CycE*, *CycA*, *dap*, *Cdk2*, and *CycD* in the PG from Myo-depleted and control cockroaches.

In controls, results indicated low levels of *dap* expression at the beginning of N5, high values in the middle, and low levels again at the end of the stage. *CdK2*, *CycE*, *CycA*, and *CycD* expression showed an inverse pattern (Fig. 4*E*), which approximately corresponds to the dynamics of cell proliferation (Fig. 3). *dap* expression in Myo-depleted cockroaches was generally dramatically reduced, whereas *CycA*, *CycD*, and *Cdk2* expression progressively decreased during N5. *CycE* expression was not significantly affected (Fig. 4*E*). Dap is a member of the mammalian p21 family of cyclin-dependent kinase inhibitors and inhibits the G1-to-S phase transition by sequestering the CycE/Cdk2 complex in a stable but inactive form (31). Induction of *dap* transcription causes a rapid accumulation of Dap protein, which inhibits CycE/Cdk2 activity and leads to G1 cell cycle arrest (32). Conversely, *dap* knockdown leads to tissue hypertrophy and cancer processes (33, 34). We propose that down-regulation of *dap* expression may have maintained cell cycle activity in the PG of Myo-depleted cockroaches, leading to cell hyperproliferation and PG hypertrophy. The *CycE*, *CycA*, and *CdK2* expression patterns in Myo-depleted cockroaches could be a product of *dap* down-regulation and the complex epistatic relationships between these factors (28, 29). General down-regulation of *CycD* expression in the PG of Myo-depleted cockroaches suggests that Myo has either a direct or indirect stimulatory effect on the expression of this cyclin. This effect differs from phenomena observed in mammals, where myostatin induces CycD degradation (30).

Myo depletion reduces the expression of ecdysteroidogenic genes in the PG

Myo depletion increased the duration of N5 (Fig. 2*A*). To study the reasons for this delay, we measured the expression of the following 4 genes, which code for ecdysone biosynthesis enzymes: neverland (*nvd*), which converts cholesterol to 7-dehydrocholesterol; phantom (*phm*) and disembodied (*dib*), which catalyze the addition of a hydroxyl group to the 25 and 22 carbon of the cholesterol side

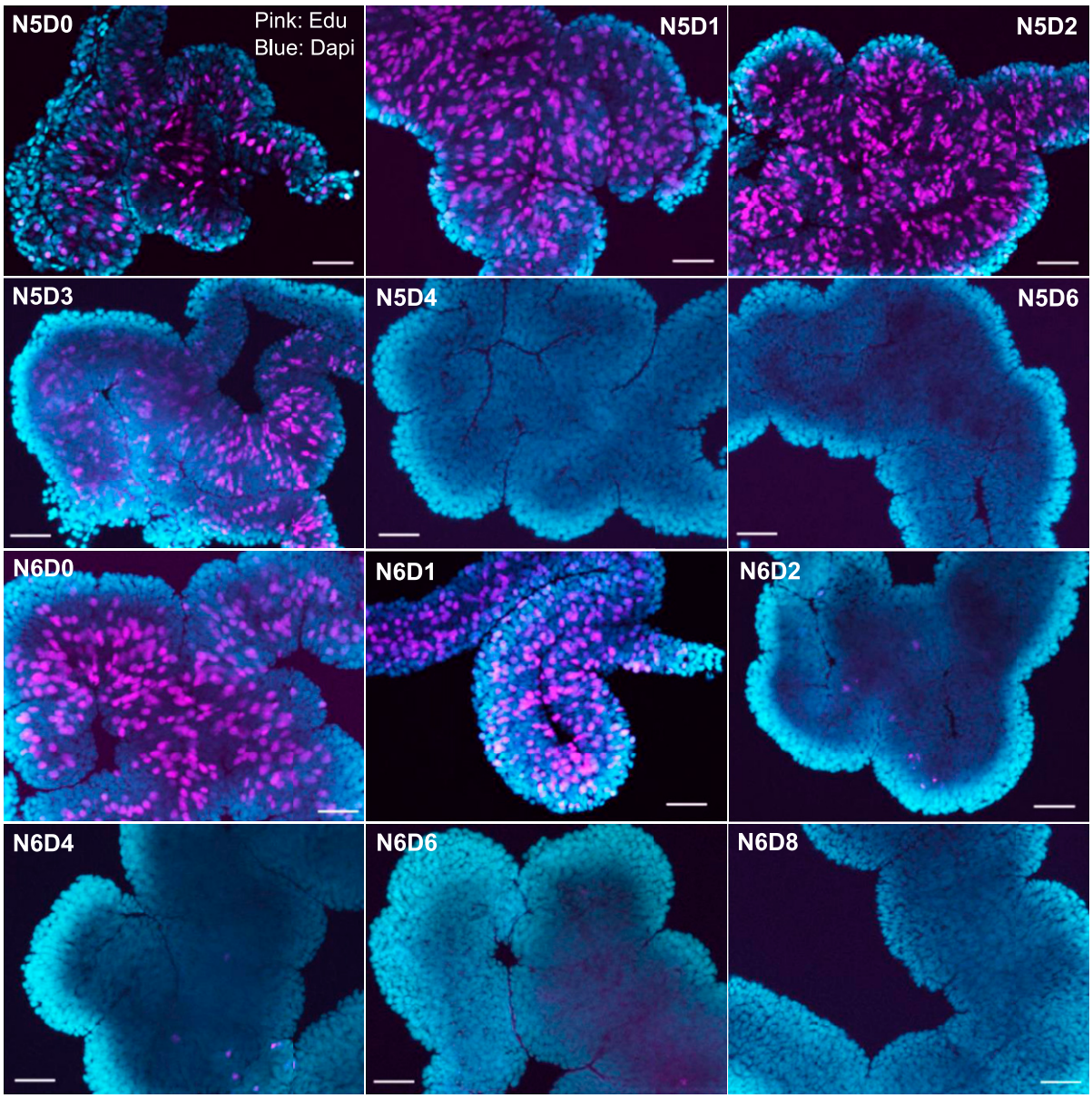

Figure 3. Cell proliferation in the PG of *B. germanica*. Double labeling EdU (discrete pink spots) and DAPI (background blue color) of PG tissue of female nymphs along the fifth and the sixth instar (from N5D0 to N5D6 and from N6D0 to N6D8). Scale bars, 50 μm.

chain, respectively; and shadow (*sad*), which catalyzes the addition of a hydroxyl group to the 2 carbon of the cholesterol ring (35). Results showed that the expression of *nvd* was dramatically down-regulated in N5D4 Myo-depleted cockroaches. The expression of *phm* and *dib* tended to be down-regulated, whereas that of *sad* was practically unaffected (**Fig. 5*A***).

In *D. melanogaster*, the activin branch of the TGF-β pathway promotes the expression of *nvd*, *dib*, and *spookier* (which is involved in catalyzing the conversion of 7-dehydrocholesterol to delta4, diketol), whereas it does not apparently affect *phm* and *sad* expression (23). These genes may be directly affected by the TGF-β pathway, or this pathway's influence could be mediated by the PTTH/torso pathway, acting at a transcriptional level, and the insulin pathway, acting post-transcriptionally (23). To date, there is no evidence that a PTTH/Torso pathway exists in cockroaches. Therefore, we focused on the insulin pathway by measuring insulin receptor (*InR*) expression, which was down-regulated in the PG from Myo-depleted cockroaches (Fig. 5*B*). If Myo has a systemic stimulatory effect on *InR* expression, it could also explain the small size of the N6 stage emerging from dsMyo-treated N5 cockroaches (Fig. 2*C*, *D*).

We propose that Myo indirectly promotes *nvd*, *phm*, and *dib* expression. The stimulatory action on *nvd* and *dib* could be mediated by the insulin pathway, as in *D. melanogaster*. In the case of *B. germanica*, however, the insulin pathway would act at a transcriptional level on these genes, rather than post-transcriptionally, as occurs in *D. melanogaster* (23). Additionally, we cannot rule out the possibility that the apparent stimulation of *phm* and *dib*

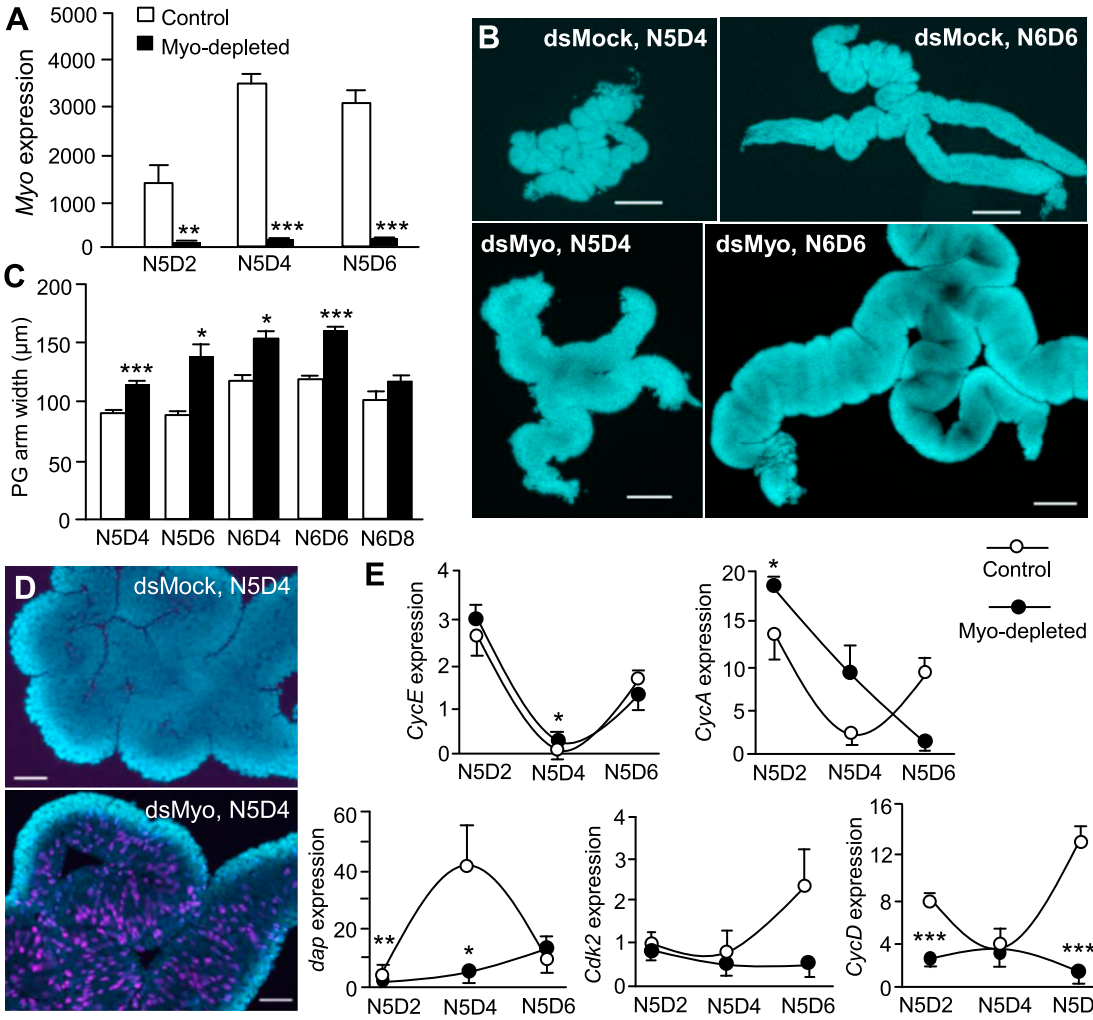

Figure 4. Effects of Myo mRNA depletion on PG growth in *B. germanica*. *A*) mRNA levels of Myo in PG of Myo-depleted cockroaches and in controls measured on 2-, 4-, and 6-d-old fifth instar female nymphs (N5D2, N5D4, and N5D6). *B*) DAPI-stained PGs from dsMock and dsMyo specimens in N5D4 at N6D6. Scale bars, 200 μm. *C*) PG arm width along different days of N5 (N5D4 and N5D6) and N6 (N6D4, N6D6, and N6D8), comparing Myo-depleted cockroaches and controls. *D*) Double-labeling EdU (discrete pink spots) and DAPI (gland background bluish color) of PGs of N5D4, comparing Myo-depleted cockroaches and controls. Scale bar, 50 μm. *E*) mRNA levels of *CycE*, *CycA*, *dap*, *Cdk2*, and *CycD* in PG tissues from dsMyo-treated cockroaches and controls on N5D2, N5D4, and N5D6. In *A* and *E*, results are indicated as copies of the given transcript per 1000 copies of BgActin-5c mRNA. In all quantitative diagrams, results are expressed as the mean ± SEM (n = 3–5). Asterisks indicate statistically significant differences with respect to controls. *$P < 0.05$, **$P < 0.01$, ***$P < 0.001$ (Student's t test).

transcription might also be mediated by fushi tarazu transcription factor 1 (FTZ-F1). Whereas FTZ-F1 enhances *phm* and *dib* expression in the ring gland from late third-stage larva of *D. melanogaster* (36), our measurements revealed that *ftz-f1* expression was delayed and down-regulated in the PG of Myo-depleted cockroaches (Fig. 5C). This supports the hypothesis that FTZ-F1 helps enhance *phm* and *dib* transcription in the PG of *B. germanica*. Finally, decreased expression of ecdysteroidogenic genes in Myo-depleted insects might be mediated by the increased expression of *jhamt* and *Kr-h1* because JH and Kr-h1 inhibit the expression of these genes (37, 38). We explored this possibility through experiments examining Myo in N6.

We also studied the expression of the ecdysone-dependent genes *E75-A*, *HR3-A*, and *ftz-f1*, which have previously been characterized in *B. germanica* (39–41). The expression pattern of these genes was conspicuously reduced (especially that of *ftz-f1*) and delayed in the PG of Myo-depleted cockroaches (Fig. 5C). This is reminiscent of the developmental delay observed in *D. melanogaster* with impaired signaling in the activin branch of the TGF-β pathway, which was due to deficient ecdysone production by the PG (23, 42). The same mechanism may explain why N5 lasts longer in Myo-depleted cockroaches (Fig. 2*B*).

Myo depletion prevents the onset of PG degeneration

In the PG of *B. germanica*, ecdysone signaling promotes the degeneration of the gland toward the end of N6 and the beginning of adult life. This is mediated by FTZ-F1, a distal transducer in the ecdysone signaling pathway that is expressed at markedly high levels in the PG in the last day of N6 (N6D8) (43). On the other hand, the inhibitor of

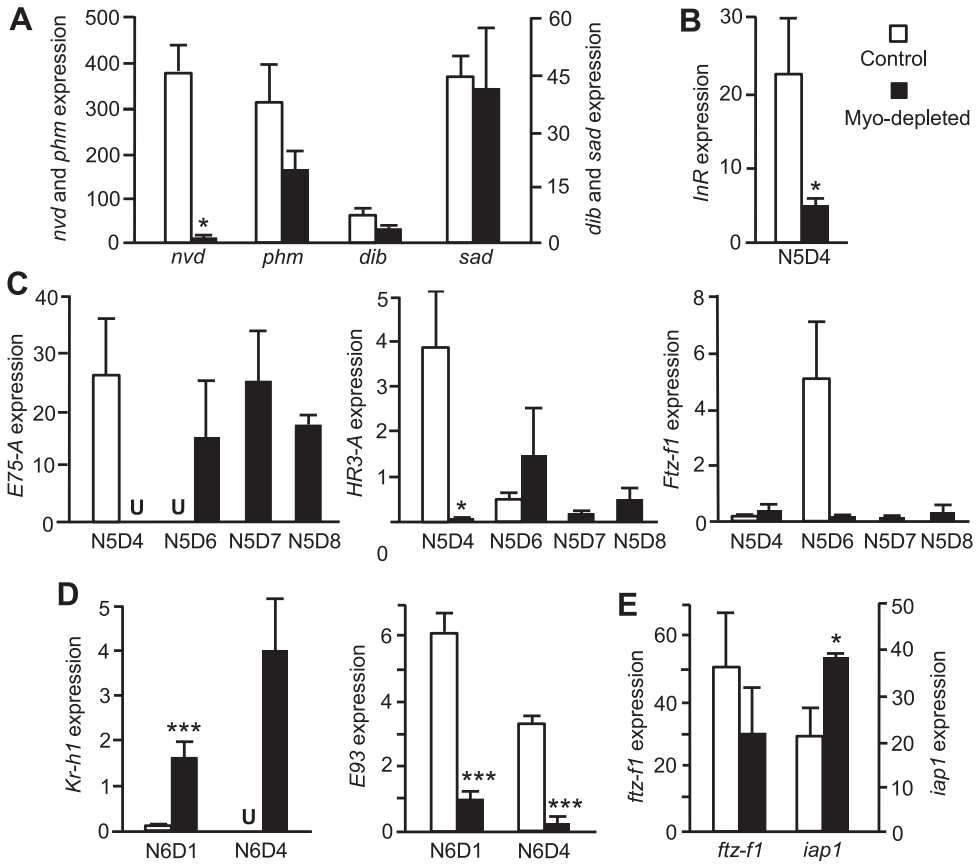

Figure 5. Effects of Myo mRNA depletion on the expression of PG factors in *B. germanica*. *A*) mRNA levels of *nvd*, *phm*, *dib*, and *sad* in PG from Myo-depleted cockroaches and controls on 4-d-old fifth instar female nymphs (N5D4). *B*) mRNA levels of *InR* in PG from Myo-depleted cockroaches and controls on N5D4. *C*) mRNA levels of *E75-A*, *HR3-A*, and *ftz-f1* in PG from Myo-depleted cockroaches and controls measured on different days of N5 (N5D4 and N5D6 in controls, and N5D4, N5D6, N5D7, and N5D8 in dsMyo-treated). *D*) mRNA levels of *Kr-h1* and *E93* in PG from Myo-depleted cockroaches and controls on N6D1 and N6D4. *E*) mRNA levels of *iap1* and *ftz-f1* in PG from Myo-depleted cockroaches and controls on N6D8. Results, indicated as copies of the given transcript per 1000 copies of BgActin-5c mRNA, are expressed as mean ± SEM ($n = 3$–5). "U" in *C* and *D* means that the expression was below the limit of detection. Asterisks indicate statistically significant differences with respect to controls. $^*P < 0.05$, $^{***}P < 0.001$ (Student's *t* test).

apoptosis-1 (IAP1) protects the PG from degeneration in early N6 and earlier nymphal stages. *iap1* shows maximal expression at N6D7 before it starts to decrease at N6D8, coinciding with a sharp peak in *ftz-f1* expression (43). JH also plays a protective role because treating N6 with the JH analog methoprene attenuates the expression of *ftz-f1* in N6D8 and prevents PG degeneration (43).

In our experiments, Myo-depleted N6 cockroaches molted to a supernumerary N7 and, in some cases, successively on to N8 and adult, indicating the PG was functional after N6. To study the mechanisms that prevented PG degeneration, we measured the expression of *Kr-h1* as a key transducer of the JH signal and *ftz-f1*, *iap1*, and *E93* as potential regulators of the onset of PG degeneration. Results showed that *Kr-h1* was up-regulated, whereas *E93* was down-regulated, in N6 Myo-depleted cockroaches (Fig. 5*D*). This presumably results from the higher production of JH in the CA, where Myo-depleted cockroaches maintained up-regulated *jhamt* expression in N6, with the consequent increase in *Kr-h1* transcription in the CA and peripheral tissues (Fig. 2*E*). Given that Kr-h1 represses *E93* expression in metamorphic tissues (3), *E93* was down-regulated in the PG (Fig. 5*D*). On the last day of N6 (N6D8), *ftz-f1* and *iap1* showed the highest and lowest expression values, respectively, within the stage (43). In the PG of Myo-depleted cockroaches, however, *ftz-f1* expression at N6D8 tended to be lower than in controls (40% on average), whereas *iap1* expression was significantly up-regulated (73% on average) (Fig. 5*E*). This is consistent with the notion that IAP1 and JH protect PG from degeneration, whereas FTZ-F1 plays a proapoptotic role (43). E93 may also be involved in PG degeneration in *B. germanica*, as it is known to have pro-apoptotic functions [for example, in the degeneration of salivary glands during *D. melanogaster* metamorphosis (44–46)], but further work would be necessary to assess this conjecture.

Myo depletion in the final nymphal stage produces the same effects as when depleted in the penultimate nymphal stage

Recent reports indicate that JH can inhibit ecdysone production in holometabolan insects, such as the fly *D. melanogaster* and the silkmoth *Bombyx mori*. The effect is mediated by Kr-h1, which represses the expression of ecdysteroidogenic genes (37, 38). Therefore, it is plausible that the reduced expression of *nvd*, *phm*, and *dib* in dsMyo-treated cockroaches could be due to an increase in *Kr-h1* expression resulting from Myo depletion (Fig. 2*E*). To study this possibility, we carried out a series of RNAi experiments injecting the dsMyo (3 μg) on the first day of the sixth (final) nymphal stage (N6D1) of *B. germanica*, when JH is practically absent (6) and *Kr-h1* expression is very low (7). The dsMyo treatment in N6D1 significantly reduced the Myo mRNA levels in

the PG, as measured on N6D2, N6D4, and N6D6 (Supplemental Fig. S3*A*). Regarding the ecdysteroidogenic enzymes, results showed that the expression of *nvd*, *phm*, and *dib* was significantly down-regulated in Myo-depleted cockroaches, as measured in N6D6, whereas that of *sad* was practically unaffected (Supplemental Fig. S3*B*). The dsMyo treatment up-regulated the expression of *Kr-h1*, and, consequently, the expression of *E93* was down-regulated (Supplemental Fig. S3*C*), as also occurred in the experiments depleting Myo in N5 (Fig. 5*D*). This could be due to an up-regulation of *jhamt* expression in the CA resulting from Myo depletion, which could result in increased production of JH affecting the expression of *Kr-h1* in peripheral tissues, like the PG. To test this conjecture, we measured the expression of *jhamt* in N6D6 in the CA of cockroaches treated with dsMyo on N6D1. We found that Myo mRNA in the CA had been significantly reduced by the treatment, and results additionally showed that *jhamt* expression was dramatically up-regulated. *Kr-h1* expression tended to be up-regulated, probably due to an increase of JH production, and *E93* tended to be down-regulated, probably as a consequence of the increased *Kr-h1* expression (Supplemental Fig. S3*D*).

In the cockroaches treated with dsMyo in N6D1, we also studied the dynamics of growth and cell proliferation in the PG using EdU labeling. Dissections of Myo-depleted cockroaches in N6D6 revealed that PG size was greater than in controls (Supplemental Fig. S4*A*). Measurement of the PG arm width in N6D2, N6D4, and N6D6 showed that, as occurred with the treatment in N5D0, the gland from Myo-depleted cockroaches grew bigger than in the controls, which was well apparent in N6D6 (Supplemental Fig. S4*B*). In N6, intense cell division in the PG is only observed on d 0 and 1 and is almost undetectable on d 2 (Fig. 3). In the dsMyo treatments on N6D1, controls showed a very faint Edu labeling in N6D2, whereas the PG from Myo-depleted cockroaches showed a very active cell division this day, which vanished 2 d later (Supplemental Fig. S4*C*).

DISCUSSION

Transcriptome data indicated that Myo expression is highly up-regulated in N5 of *B. germanica*. This general up-regulation in N5 is consistent with our present results obtained by means of real-time quantitative PCR, which show high levels of Myo expression at the beginning of N5 in the CC–CA and toward the mid-end of N5 in the PG.

Our present results also indicate that high Myo levels in N5 repress *jhamt* expression in the CC–CA, which results in a reduction in JH production at the beginning of N6 (**Fig. 6**). In juvenile stages, JH, acting through Kr-h1, represses the expression of *ftz-f1*, which is a repressor of *iap1* expression in the PG. In N6, low levels of circulating JH result in lower *Kr-h1* expression in the PG, with the concomitant de-repression of *ftz-f1* expression, inhibition of *iap1*, and activation of the caspase-mediated gland degeneration mechanisms (Fig. 6). Because *E93* is a gene activated by ecdysone signaling, is a typical apoptosis-triggering factor and is repressed by Kr-h1, we conjecture that the proapoptotic action of FTZ-F1 might be mediated by E93 (Fig. 6).

In the PG, Myo is expressed during N5 and N6, but there is a marked peak of expression toward the mid-end of N5. Our data indicate that high expression of *myo* correlates with high expression of ecdysone biosynthesis genes like *nvd*, *phm*, and *dib*. This may be due to the inhibition of Myo on *jhamt* expression, and thus on JH production and concomitant *Kr-h1* expression, because Kr-h1 has been shown to repress the expression of ecdysteroidogenic enzyme genes (37, 38). In any case, the high expression of Myo in N5 surely contributes to the production of the large, metamorphic ecdysone pulse in N6. The data also suggest that the peak of Myo expression in N5 helps repress cell proliferation (at least in part by enhancing the expression of *dap*). Control over cell proliferation in N6 may be required to produce the subsequent metamorphic ecdysone pulse (Fig. 6).

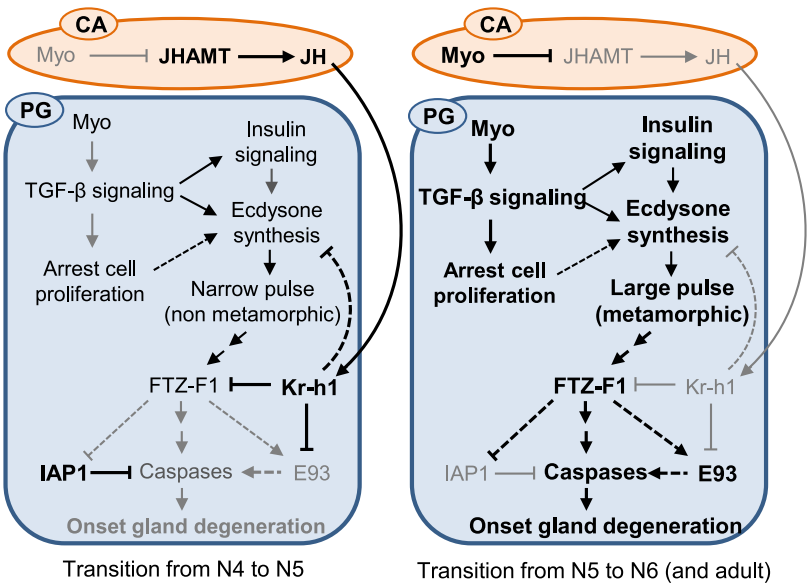

Figure 6. Roles of Myo in the CA and the PG in the transition to the pre-metamorphic stage of *B. germanica*. High levels of the indicated factors and corresponding interactions and final processes are indicated in bold; low levels are indicated in gray. Continuous lines indicate interactions suggested by the experiments. Dashed lines indicate interactions hypothesized.

Our overall findings point to Myo as a key trigger of the transition from penultimate to final (pre-metamorphic) nymphal stage in *B. germanica*. The repressor role of Myo on *jhamt* expression and JH production has previously been reported in the cricket *G. bimaculatus* (14). Although the functions of Myo in the PG were not examined in this insect, Ishimaru *et al.* (14) reported that Myo expression levels were high in this gland. We presume, therefore, that the trigger role Myo plays in the pre-metamorphic stage of *B. germanica* may be extended to *G. bimaculatus* and perhaps to other hemimetabolan insects. Myo expression in *D. melanogaster* does not exhibit an especially prominent peak during the larval and pupa stages in the Northern blot analyses published by Lo and Frasch (11) or in the transcriptome profiles reported by us (10). The larva–pupa–adult transition in the holometabolan metamorphosis requires a relatively rapid pattern of decreasing–increasing–decreasing JH production (2, 47). In this context, a dramatic interruption of JH production mediated by the repressive action of Myo on CA *jhamt* expression might not be suited for regulating metamorphosis in holometabolan species. We conclude that the role of Myo as a pre-metamorphosis trigger, at least in relation to the action in the CA and to JH, might be restricted to hemimetabolan insects, and this mechanism may have been lost in the evolutionary transition from hemimetaboly to holometaboly. FJ

ACKNOWLEDGMENTS

The authors thank Guillem Ylla and Jose Carlos Montañes [both from the Institute of Evolutionary Biology (IBE), Spanish National Research Council-Universitat Pompeu Fabra] for helping with transcriptome comparisons and searching for genes in the *B. germanica* genome (available at *https://www.hgsc.bcm.edu/arthropods/german-cockroach-genomeproject*) as provided by the Baylor College of Medicine Human Genome Sequencing Center; Alba Ventos-Alfonso (IBE) for helping with different experiments and image treatment; and Maria-Dolors Piulachs and Jose-Luis Maestro (IBE) for helpful discussions. This work was supported by Spanish Ministry of Economy and Competitiveness Grants CGL2012–36251 and CGL2015–64727-P (to X.B.), by Catalan Government Grant 2017 SGR 1030 (to X.B.), and by the European Fund for Economic and Regional Development (FEDER funds). O.K. received a Royal Thai Government Scholarship to do a PhD thesis in X.B. laboratory, Barcelona. The authors declare no conflicts of interest.

AUTHOR CONTRIBUTIONS

X. Belles designed the research; O. Kamsoi performed the RNAi experiments and the real-time quantitative PCR measurements; O. Kamsoi and X. Belles analyzed the data; O. Kamsoi drafted a first version of the manuscript; and X. Belles wrote the final version of the manuscript.

REFERENCES

1. Nijhout, H. F. (1994) *Insect Hormones*, Princeton University Press, Princeton, NJ, USA
2. Jindra, M., Palli, S. R., and Riddiford, L. M. (2013) The juvenile hormone signaling pathway in insect development. *Annu. Rev. Entomol.* **58**, 181–204
3. Belles, X., and Santos, C. G. (2014) The MEKRE93 (Methoprene tolerant-Krüppel homolog 1-E93) pathway in the regulation of insect metamorphosis, and the homology of the pupal stage. *Insect Biochem. Mol. Biol.* **52**, 60–68
4. Jindra, M., Uhlirova, M., Charles, J.-P., Smykal, V., and Hill, R. J. (2015) Genetic evidence for function of the bHLH-PAS protein Gce/Met as a juvenile hormone receptor. *PLoS Genet.* **11**, e1005394
5. Jindra, M., Bellés, X., and Shinoda, T. (2015) Molecular basis of juvenile hormone signaling. *Curr. Opin. Insect Sci.* **11**, 39–46
6. Treiblmayr, K., Pascual, N., Piulachs, M.-D., Keller, T., and Belles, X. (2006) Juvenile hormone titer versus juvenile hormone synthesis in female nymphs and adults of the German cockroach, *Blattella germanica*. *J. Insect Sci.* **6**, 1–7
7. Lozano, J., and Belles, X. (2011) Conserved repressive function of Krüppel homolog 1 on insect metamorphosis in hemimetabolous and holometabolous species. *Sci. Rep.* **1**, 163
8. Belles, X. (2017) MicroRNAs and the evolution of insect metamorphosis. *Annu. Rev. Entomol.* **62**, 111–125
9. Lozano, J., Montañez, R., and Belles, X. (2015) MiR-2 family regulates insect metamorphosis by controlling the juvenile hormone signaling pathway. *Proc. Natl. Acad. Sci. USA* **112**, 3740–3745
10. Ylla, G., Piulachs, M. D., and Belles, X. (2018) Comparative transcriptomics in two extreme neopterans reveals general trends in the evolution of modern insects. *iScience* **4**, 164–179
11. Lo, P. C., and Frasch, M. (1999) Sequence and expression of myoglianin, a novel *Drosophila* gene of the TGF-beta superfamily. *Mech. Dev.* **86**, 171–175
12. Peterson, A. J., and O'Connor, M. B. (2014) Strategies for exploring TGF-β signaling in *Drosophila*. *Methods* **68**, 183–193
13. Awasaki, T., Huang, Y., O'Connor, M. B., and Lee, T. (2011) Glia instruct developmental neuronal remodeling through TGF-β signaling. *Nat. Neurosci.* **14**, 821–823
14. Ishimaru, Y., Tomonari, S., Matsuoka, Y., Watanabe, T., Miyawaki, K., Bando, T., Tomioka, K., Ohuchi, H., Noji, S., and Mito, T. (2016) TGF-β signaling in insects regulates metamorphosis via juvenile hormone biosynthesis. *Proc. Natl. Acad. Sci. USA* **113**, 5634–5639
15. Huang, J., Tian, L., Peng, C., Abdou, M., Wen, D., Wang, Y., Li, S., and Wang, J. (2011) DPP-mediated TGFbeta signaling regulates juvenile hormone biosynthesis by activating the expression of juvenile hormone acid methyltransferase. *Development* **138**, 2283–2291
16. Ciudad, L., Piulachs, M.-D., and Bellés, X. (2006) Systemic RNAi of the cockroach vitellogenin receptor results in a phenotype similar to that of the *Drosophila* yolkless mutant. *FEBS J.* **273**, 325–335
17. Chehrehasa, F., Meedeniya, A. C. B., Dwyer, P., Abrahamsen, G., and Mackay-Sim, A. (2009) EdU, a new thymidine analogue for labelling proliferating cells in the nervous system. *J. Neurosci. Methods* **177**, 122–130
18. Misof, B., Liu, S., Meusemann, K., Peters, R. S., Donath, A., Mayer, C., Frandsen, P. B., Ware, J., Flouri, T., Beutel, R. G., Niehuis, O., Petersen, M., Izquierdo-Carrasco, F., Wappler, T., Rust, J., Aberer, A. J., Aspöck, U., Aspöck, H., Bartel, D., Blanke, A., Berger, S., Böhm, A., Buckley, T. R., Calcott, B., Chen, J., Friedrich, F., Fukui, M., Fujita, M., Greve, C., Grobe, P., Gu, S., Huang, Y., Jermiin, L. S., Kawahara, A. Y., Krogmann, L., Kubiak, M., Lanfear, R., Letsch, H., Li, Y., Li, Z., Li, J., Lu, H., Machida, R., Mashimo, Y., Kapli, P., McKenna, D. D., Meng, G., Nakagaki, Y., Navarrete-Heredia, J. L., Ott, M., Ou, Y., Pass, G., Podsiadlowski, L., Pohl, H., von Reumont, B. M., Schütte, K., Sekiya, K., Shimizu, S., Slipinski, A., Stamatakis, A., Song, W., Su, X., Szucsich, N. U., Tan, M., Tan, X., Tang, M., Tang, J., Timelthaler, G., Tomizuka, S., Trautwein, M., Tong, X., Uchifune, T., Walzl, M. G., Wiegmann, B. M., Wilbrandt, J., Wipfler, B., Wong, T. K. F., Wu, Q., Wu, G., Xie, Y., Yang, S., Yang, Q., Yeates, D. K., Yoshizawa, K., Zhang, Q., Zhang, R., Zhang, W., Zhang, Y., Zhao, J., Zhou, C., Zhou, L., Ziesmann, T., Zou, S., Li, Y., Xu, X., Zhang, Y., Yang, H., Wang, J., Wang, J., Kjer, K. M., and Zhou, X. (2014) Phylogenomics resolves the timing and pattern of insect evolution. *Science* **346**, 763–767
19. Ureña, E., Manjón, C., Franch-Marro, X., and Martín, D. (2014) Transcription factor E93 specifies adult metamorphosis in hemimetabolous and holometabolous insects. *Proc. Natl. Acad. Sci. USA* **111**, 7024–7029
20. Santos, C. G., Fernandez-Nicolas, A., and Belles, X. (2016) Smads and insect hemimetabolan metamorphosis. *Dev. Biol.* **417**, 104–113
21. Peterson, A. J., and O'Connor, M. B. (2013) Activin receptor inhibition by Smad2 regulates *Drosophila* wing disc patterning through BMP-response elements. *Development* **140**, 649–659

22. Zheng, X., Wang, J., Haerry, T. E., Wu, A. Y.-H., Martin, J., O'Connor, M. B., Lee, C.-H. J., and Lee, T. (2003) TGF-beta signaling activates steroid hormone receptor expression during neuronal remodeling in the *Drosophila* brain. *Cell* **112**, 303–315
23. Gibbens, Y. Y., Warren, J. T., Gilbert, L. I., and O'Connor, M. B. (2011) Neuroendocrine regulation of Drosophila metamorphosis requires TGFbeta/Activin signaling. *Development* **138**, 2693–2703
24. Romañá, I., Pascual, N., and Belles, X. (1995) The ovary is a source of circulating ecdysteroids in *Blattella germanica* (Dictyoptera: Blattellidae). *Eur. J. Entomol.* **93**, 93–103
25. Cruz, J., Martín, D., Pascual, N., Maestro, J. L., Piulachs, M. D., and Bellés, X. (2003) Quantity does matter. Juvenile hormone and the onset of vitellogenesis in the German cockroach. *Insect Biochem. Mol. Biol.* **33**, 1219–1225
26. Chiang, A.-S., Tsai, W.-H., and Schal, C. (1995) Neural and hormonal regulation of growth of corpora allata in the cockroach, Diploptera punctata. *Mol. Cell. Endocrinol.* **115**, 51–57
27. Sakurai, S. (2005) Feedback regulation of prothoracic gland activity. In *Comprehensive Molecular Insect Science* (Gilbert, L. I., Iatrou, K., and and Gill, S. S., eds.), pp. 409–431, Elsevier Pergamon, San Diego, CA, USA
28. Barr, A. R., Heldt, F. S., Zhang, T., Bakal, C., and Novák, B. (2016) A dynamical framework for the all-or-none G1/S transition. *Cell Syst.* **2**, 27–37
29. Bertoli, C., Skotheim, J. M., and de Bruin, R. A. M. (2013) Control of cell cycle transcription during G1 and S phases. *Nat. Rev. Mol. Cell Biol.* **14**, 518–528
30. Yang, W., Zhang, Y., Li, Y., Wu, Z., and Zhu, D. (2007) Myostatin induces cyclin D1 degradation to cause cell cycle arrest through a phosphatidylinositol 3-kinase/AKT/GSK-3 beta pathway and is antagonized by insulin-like growth factor 1. *J. Biol. Chem.* **282**, 3799–3808
31. Lane, M. E., Sauer, K., Wallace, K., Jan, Y. N., Lehner, C. F., and Vaessin, H. (1996) Dacapo, a cyclin-dependent kinase inhibitor, stops cell proliferation during *Drosophila* development. *Cell* **87**, 1225–1235
32. Swanson, C. I., Meserve, J. H., McCarter, P. C., Thieme, A., Mathew, T., Elston, T. C., and Duronio, R. J. (2015) Expression of an S phase-stabilized version of the CDK inhibitor Dacapo can alter endoreplication. *Development* **142**, 4288–4298
33. Nakayama, K., Ishida, N., Shirane, M., Inomata, A., Inoue, T., Shishido, N., Horii, I., Loh, D. Y., and Nakayama, K. (1996) Mice lacking p27(Kip1) display increased body size, multiple organ hyperplasia, retinal dysplasia, and pituitary tumors. *Cell* **85**, 707–720
34. Kiyokawa, H., Kineman, R. D., Manova-Todorova, K. O., Soares, V. C., Hoffman, E. S., Ono, M., Khanam, D., Hayday, A. C., Frohman, L. A., and Koff, A. (1996) Enhanced growth of mice lacking the cyclin-dependent kinase inhibitor function of p27(Kip1). *Cell* **85**, 721–732
35. Niwa, R., and Niwa, Y. S. (2014) Enzymes for ecdysteroid biosynthesis: their biological functions in insects and beyond. *Biosci. Biotechnol. Biochem.* **78**, 1283–1292
36. Parvy, J.-P., Blais, C., Bernard, F., Warren, J. T., Petryk, A., Gilbert, L. I., O'Connor, M. B., and Dauphin-Villemant, C. (2005) A role for betaFTZ-F1 in regulating ecdysteroid titers during post-embryonic development in *Drosophila melanogaster*. *Dev. Biol.* **282**, 84–94
37. Liu, S., Li, K., Gao, Y., Liu, X., Chen, W., Ge, W., Feng, Q., Palli, S. R., and Li, S. (2018) Antagonistic actions of juvenile hormone and 20-hydroxyecdysone within the ring gland determine developmental transitions in *Drosophila*. *Proc. Natl. Acad. Sci. USA* **115**, 139–144
38. Zhang, T., Song, W., Li, Z., Qian, W., Wei, L., Yang, Y., Wang, W., Zhou, X., Meng, M., Peng, J., Xia, Q., Perrimon, N., and Cheng, D. (2018) Krüppel homolog 1 represses insect ecdysone biosynthesis by directly inhibiting the transcription of steroidogenic enzymes. *Proc. Natl. Acad. Sci. USA* **115**, 3960–3965
39. Mané-Padrós, D., Cruz, J., Vilaplana, L., Pascual, N., Bellés, X., and Martín, D. (2008) The nuclear hormone receptor BgE75 links molting and developmental progression in the direct-developing insect *Blattella germanica*. *Dev. Biol.* **315**, 147–160
40. Cruz, J., Martín, D., and Bellés, X. (2007) Redundant ecdysis regulatory functions of three nuclear receptor HR3 isoforms in the direct-developing insect *Blattella germanica*. *Mech. Dev.* **124**, 180–189
41. Cruz, J., Nieva, C., Mané-Padrós, D., Martín, D., and Bellés, X. (2008) Nuclear receptor BgFTZ-F1 regulates molting and the timing of ecdysteroid production during nymphal development in the hemimetabolous insect *Blattella germanica*. *Dev. Dyn.* **237**, 3179–3191
42. Brummel, T., Abdollah, S., Haerry, T. E., Shimell, M. J., Merriam, J., Raftery, L., Wrana, J. L., and O'Connor, M. B. (1999) The *Drosophila* activin receptor baboon signals through dSmad2 and controls cell proliferation but not patterning during larval development. *Genes Dev.* **13**, 98–111
43. Mané-Padrós, D., Cruz, J., Vilaplana, L., Nieva, C., Ureña, E., Bellés, X., and Martín, D. (2010) The hormonal pathway controlling cell death during metamorphosis in a hemimetabolous insect. *Dev. Biol.* **346**, 150–160
44. Baehrecke, E. H., and Thummel, C. S. (1995) The *Drosophila* E93 gene from the 93F early puff displays stage- and tissue-specific regulation by 20-hydroxyecdysone. *Dev. Biol.* **171**, 85–97
45. Lee, C. Y., Wendel, D. P., Reid, P., Lam, G., Thummel, C. S., and Baehrecke, E. H. (2000) E93 directs steroid-triggered programmed cell death in *Drosophila*. *Mol. Cell* **6**, 433–443
46. Lee, C. Y., and Baehrecke, E. H. (2001) Steroid regulation of autophagic programmed cell death during development. *Development* **128**, 1443–1455
47. Belles, X. (2011) Origin and evolution of insect metamorphosis. In *Encyclopedia of Life Sciences (ELS)*, John Wiley & Sons, Ltd, Chichester, United Kingdom

Received for publication July 23, 2018.
Accepted for publication October 22, 2018.